IASJ

المجلات الاكاديمية العراقية

Tikrit Journal of Pure Science

ISSN: 1813 – 1662 (Print) --- E-ISSN: 2415 – 1726 (Online)

Journal Homepage: http://tjps.tu.edu.iq/index.php/j

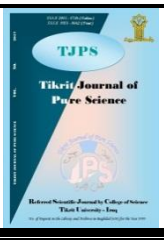

Study effect of window and BSF layers on the properties of the CZTS / CZTSe solar cell by SCAPS–1D

Alaa H. Najim , Ayed N. Saleh

Department of physics , Collage of Education for pure science , Tikrit University , Tikrit , Iraq

https://doi.org/10.25130/tjps.v24i3.372

ARTICLE INFO.

Article history:

-Received: 30 / 9 / 2018

-Accepted: 12 / 11 / 2018

-Available online: / / 2019

Keywords: SCAPS-1D, CZTSe, CZTS, transition metal oxides (TMO), Back surface field (BSF), solar cell, conversion efficiency (η), fill factor (FF), Quantum efficiency (QE).

Corresponding Author:

Name: Ayed N. Saleh

E-mail: ayed.ns@tu.edu.iq

Tel:

ABSTRACT

The solar cell CZTS / CZTSe was studied using SCAPS-1D * computer simulator. It was noted that increasing the thickness of the absorber layer p-CZTSe from 250nm to 5µm leads to increase the IV curve. thus increasing the values of Voc, Jsc, FF, η up to 0.79 Volt, 39.35 mA/cm^2, 85.92% and 26.8% respectively, and optical properties of Quantum efficiency (QE) increased from 54% to 95%. The addition of the transition metal oxides (TMO) to the cell showed that the oxides (TiO_2 , SnO_2 , ITO, FTO) had the highest conversion efficiency among the other oxides at 25.63% and this value increased by increasing the thickness of the absorption layer to 29.32%. In addition to the BSF of the cell , p^+-CdTe, SnS, had the highest conversion efficiency of 33.75% and 29.64%, respectively. The thickness of the absorption layer increased the conversion efficiency value from 13.16% at 250nm to 33.9 5% at 5µm for p^+-CdTe, and from 10.27% to 29.89% for SnS, While the value of the fill factor (FF) is reduced from 69.93% at 250 nm to 61.01% at 2 µm for p^+-CdTe, and at most constant value at 85 % for SnS. By combining these compounds from the transition metal oxides and the Back surface field with the CZTS / CZTSe cell, Can get six cells with conversion efficiency values ranging between 33.82% and 29.71%, and the change in these values can affect the thickness by change the thickness of the absorption layer. For quantum efficiency, their value is increased to 100% by the rise in the absorption layer thickness to 5µm because cells are ideal .

Introduction

Solar cells are photovoltaic devices that convert electromagnetic radiation (i.e. light, including infrared, visible and ultraviolet radiation) from the sun to usable electrical energy. Solar cells are used in various terrestrial and space applications, as they can convert solar energy directly into electrical energy, with good conversion efficiency, and can produce near-constant capacity, low operating costs and no pollution in the environment [1]. The study of binary compounds has increased the creation of new materials for solar cells. The research has focused on thin film solar cells for high efficiency and relatively low cost. Currently, the semiconductors Cu2ZnSnSe4 (CZTSe), Cu2ZnSnS4 (CZTS) and their alloys Cu_2ZnSn ($S_{1-x}Se_x$) 4 with the direct power gap between (1-1.5 eV) attract attention [2]. Because they contain abundant and safe elements such as Zn and Sn, and the coefficient of absorption of the thin film CZTSSe is large enough ($> 10^4 cm^{-1}$).The highest efficiency of the CZTSSe cell achieved so far is 12.7% where it is still far from the theoretical calculations. It is also required to understand and fully control the various manufacturing processes and interactions in order to obtain high efficiency [3]. The aim of this study is to show a high efficiency of the CZTS / CZTSe cell using the computer simulation method of solar cells in addition to studying the effect of the transition metal oxides (TMO) on the cell and the extent of their interaction with different types of these oxides to choose the best ones in terms of efficiency in addition to the use of different types of Back surface field (BSL) to see how they affect the cell.

Simulation process

The digital simulation technology of solar cell devices has proven over the years that it is an effective tool for studying and understanding the properties of solar cell devices such as optical, electrical and mechanical properties of complex solar cell devices. It also helps reduce processing costs and time spent in manufacturing solar cell devices by providing useful information on how to change production parameters to improve device performance. And we deal in this study with SCAPS-1D program, a one-dimensional solar cell simulation program developed in Electronics and information systems (ELIS), the University of Gent in Belgium and freely available to the PV research community. Where the user can describe a solar cell as a stack up to seven layers with different properties, such as thickness, optical absorption, doping, density and distribution of defects. A number of common measurements can be simulated, such as I-V, QE, C-V, and C-f. The program is available free of charge for various types of PV research. The SCAPS simulation relies on the solution of three semiconductor equations: the Poisson equation, the electron and hole continuity equation. SCAPS numerically solves these three partial differential equations, which approach the concentration of electrons and the electrostatic voltage as a function in position x. The study focused on the design of the cell as in Fig. 1 and using the absorption layer parameters and the Back surface field listed in Table (1) and the BSF mentioned in Table (2). The cells have been studied are ideal cells without defects because defects are usually added to increase electrical conductivity or to control life span, but defects are often in the factor as factor loss and therefore a high concentration of defects may reduce conversion efficiency. The temperature that has been studied in our simulation is 300 K . The QE and the I-V curve, which include the values of Voc , Jsc and FF, Find them by equations (1, 2, 3, 4), respectively.[4]

$$V_{oc} = \frac{K_B T}{q} \ln\left(\frac{J_{ph}}{J_o} + 1\right) \quad \text{.....(1)}$$

Where the Voc is the voltage in which no current flows through the external circuit when the solar cell's ends are not connected to each other, and this is the maximum voltage that the solar cell can provide. $V_{oc}$is based on the J_{ph} is Intensity of photo current of the cell and the saturation current J_o [5].

$$J_{sc}(V) = J(V) + J_o \left(e^{qV/mK_BT} - 1\right) \quad \text{...} \quad (2)$$

The short circuit current Jsc is the maximum current generated by the solar cell when the solar cell ends are in contact with one another. while V is the voltage across the junction, T is the absolute temperature, J_o is the saturation current during dark and J(V) is the net current density while m is the ideal factor with values between 1 and 2 [5].

$$FF = \frac{J_{mp} \times V_{mp}}{V_{oc}\ J_{sc}} = \frac{P_{max}}{V_{oc}\ J_{sc}} \quad \text{.....(3)}$$

The fill factor FF which is the ratio between the maximum power ($P_{max} = J_{mp} \times V_{mp}$) generated by a solar cell and the output Voc and Jsc .

$$\eta = \frac{P_{max}}{P_{in}} = \frac{J_{sc}\ V_{oc}\ FF}{P_{in}} \quad \text{.....(4)}$$

While the conversion efficiency η is described as the ratio between the maximum power generated by the cell and the power incident on it. The P_{in} radiation value of 1000 W/m^{2}of the **1.5AM** spectrum has become a standard for measuring the conversion efficiency of solar cells [4].

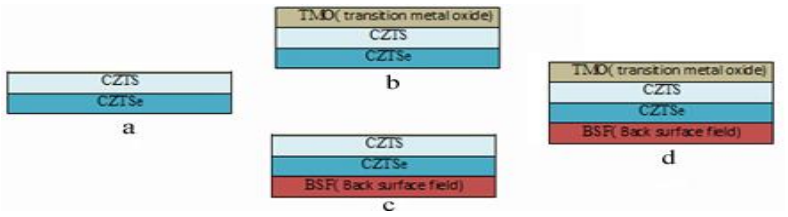

Figure (1) Stages of study and design of the cell CZTS / CZTSe

a)- HJ CZTS/CZTSe without WL and BSF b)- Solar cell with WL d)- Solar cell with BSF c)- Solar cell with WL and BSF

Table (1) Basic parameters of absorption layer and the transition metal oxides (TMO)

Parameter	symbol (unit)	ZnO [6]	TiO2 [7]	V_2O_5	CdO	SnO_2 [13]	ITO [14]	AZO [15]	ZTO [16]	FTO [17]	CZTSe [18]	CZTS [19,14]
Band gap	Eg (ev)	3.3	3.26	2.3	2.28 [9]	3.6	3.6	3.4	3.35	4.20	1	1.5
Electron affinity	χ (ev)	4.6	4.2	3.99 [5]	4.5 [10]	4.4	4.1	4.6	4.5	4.50	4.6	4.5
Dielectric permittivity	ϵ/ϵ_r	9	10	4.28	5.3 [9]	9.0	10	9	9	10	8.6	10
CB effective density of states	Nc (cm^{-3})	2.2 E+18	2 E+17	2.2 E+18	2.2 E+18	2.2 E+19	2 E+18	4 E+18	2.1 E+18	1.2 E+20	7.9 E+17	2.2 E+18
VB effective density of states	Nv (cm^{-3})	1.8 E+19	6 E+17	1.8 E+19	1.8 E+19	2 E+19	1.8 E+19	9 E+18	1.5 E+19	7.0 E+20	4.5 E+18	1.8 E+19
Electron thermal velocity	Vn(cm/s)	1.0 E+7	1 E+7	1.0 E+7	1.0 E+7	1.0 E+7	1.0 E+7	1.0 E+7	1.0 E+7	1 E+7	1.0 E+7	1.0 E+7
Hole thermal velocity	Vp(cm/s)	1.0 E+7	1 E+7	1.0 E+7	1.0 E+7	1.0 E+7	1.0 E+7	1.0 E+7	1.0 E+7	1E+7	1.0 E+7	1.0 E+7
Electron mobility	μ_n ($cm^2/v.s$)	100	1 E+2	1.26 [6]	146 [11]	1.2 E+2	50	100	52	20	40	100
Hole mobility	μ_p ($cm^2/v.s$)	25	25	34.5 [8]	39.5 [12]	3 E+1	75	31	3	100	12.6	25
absorption Coefficient	$\alpha(cm^{-1}ev^{1/2})$	1 E+5	1 E+3	1 E+5	1 E+5	1 E+5	1 E+5	1 E+5	1 E+5	1 E+5	2 E+4	2 E+4

Table (2) Basic parameters of the Back surface field (BSF)

Parameter	symbol (unit)	$MoSe_2$]20[	Si]20[	SnS]21[	P^+-CdTe [22]	Cu_2Te [22]	ZnTe [22]
Band gap	E_g (ev)	1.060	1.12	1.25	1.45	1.18	2.26
Electron affinity	χ (ev)	4.372	4.05	4.20	4.28	4.20	3.65
Dielectric permittivity	ϵ/ϵ_r	13.6	11.9	10	10	10	14
CB effective density of states	N_c (cm^{-3})	2.2 E+18	2.8 E+19	2.2 E+18	7.9 E+17	7.8 E+17	7.8 E+17
VB effective density of states	N_v (cm^{-3})	1.8 E+19	2.65 E+19	1.8 E+19	1.8 E+19	1.6 E+19	1.6 E+19
Electron thermal velocity	V_n (cm/s)	1.0 E+7	1.0 E+7	1.0 E+7	1.0 E+7	1.0 E+7	1.0 E+7
Hole thermal velocity	V_p (cm/s)	1.0 E+7	1.0 E+7	1.0 E+7	1.0 E+7	1.0 E+7	1.0 E+7
Electron mobility	μ_n $(cm^2/v.s)$	100	1450	25	110	500	100
Hole mobility	μ_p $(cm^2/v.s)$	25	500	100	70	100	10
absorption Coefficient	α $(cm^{-1}ev^{1/2})$	1 E+5	1 E+5	1 E+5	1 E+5	1 E+5	1 E+5

Results and discussion

As shown in Figure (1) , the study of CZTS / CZTSe has been divided into four main stages: the first phase of a CZTS / CZTSe study is done on its own and without any other layers to determine its properties. The second phase consists of a study of the cell and the transition metal oxides used as a window layer to determine their effect on the cell, the curve (I-V) and the quantitative efficiency (QE). The third phase include a study of the effect of the BSF on the cell and the extent to which the changes are met by the CZTS / CZTSe cell. The fourth and final stage comprise of the CZTS / CZTSe cell with the best transition layer of the transition metal oxides (TMO), as well as the best layer of BSF, to produce a high specification cell and study it. This is the main objective of the research. As shown in Table (3), the results were obtained after the thickness of the P-CZTSe absorption layer was fixed at 4μm, the thickness of the transition metal oxides (TMO) at 20 nm and the thickness of the BSF at 2μm.

Table (3) Results obtained at each stage of design of the cell CZTS / CZTSe

Layers	(v)Voc	Sc (mA/cm2)J	FF(%)	η(%)
n- CZTS / p-CZTSe	0.7860	37.905582	85.81	25.57
n-ZnO / n- CZTS / p-CZTSe	0.7860	37.799255	85.82	25.49
n-TiO2 / n- CZTS / p-CZTSe	0.7861	37.993512	85.82	25.63
n- V2O5 / n- CZTS / p-CZTSe	0.7871	38.058619	79.85	23.92
n-CdO / n- CZTS / p-CZTSe	0.7861	37.968833	85.82	25.61
n- SnO2 / n- CZTS / p-CZTSe	0.7861	37.989605	85.82	25.63
n- ITO / n- CZTS / p-CZTSe	0.7861	37.994480	85.81	25.63
n- AZO / n- CZTS / p-CZTSe	0.7861	37.961253	85.82	25.61
n-ZTO / n- CZTS / p-CZTSe	0.7861	37.961766	85.82	25.61
n- FTO / n- CZTS / p-CZTSe	0.7861	37.993475	85.82	25.63
n- CZTS / p-CZTSe / p-Si	0.7699	38.077684	85.53	25.07
n- CZTS / p-CZTSe / p-MoSe2	0.823	37.73007	83.84	21.58
n- CZTS / p-CZTSe / p-SnS	0.7911	43.936783	85.29	29.64
n- CZTS / p-CZTSe / p-CdTe	1.2280	44.933481	61.17	33.75
n- CZTS / p-CZTSe / p-Cu_2Te	0.7435	40.090612	85.13	25.37
n- CZTS / p-CZTSe / p-ZnTe		44.961488		35.95
n-TiO2 / n- CZTS / p-CZTSe/ p-CdTe	1.2274	45.021609	61.20	33.82
n-TiO2 / n- CZTS / p-CZTSe/ p-SnS	0.7911	44.024867	85.29	29.71
n- SnO2 / n- CZTS / p-CZTSe/ p-CdTe	1.2276	45.016609	61.19	33.82
n- SnO2 / n- CZTS / p-CZTSe/ p-SnS	0.7911	44.020023	85.29	29.70
n- ITO / n- CZTS / p-CZTSe/ p-CdTe	1.2269	45.021486	61.23	33.82
n- ITO / n- CZTS / p-CZTSe/ p-SnS	0.7911	44.024899	85.28	29.70
n- FTO / n- CZTS / p-CZTSe/ p-CdTe	1.2276	45.021625	61.20	33.82
n- FTO / n- CZTS / p-CZTSe/ p-SnS	0.7911	44.024876	85.29	29.71

Table (3) shows that TiO2, SnO2, ITO, and FTO compounds have the highest conversion efficiency among the other transition metal oxides (25.63%) and are therefore selected in the final cell design. The compound (CdTe) has the highest conversion efficiency among the other back reflection layers (33.75%), but the FF value for this compound is small (61.17%). So SnS was selected with the conversion efficiency value of 29.64% . Finally, the cell (TiO2 or SnO2 or ITO or FTO)/ CZTS / CZTSe/ (CdTe or SnS) was obtained to study the change in thickness of the absorption layer CZTSe on the properties curve (IV) and QE after having achieved the efficiency value Conversion (η) between (29.7%) and (33.82%).

Figure (2) present that the window layers (WL) have no effect on the I-V properties curve except V_2O_5 , which has slightly changed the shape of the curve .

And figure (3) illustrates that the addition of the Back surface field (BSF) has caused a significant change in the shape of the I-V curve and that CdTe has the highest increase in the curve. The rise in energy absorption can lead to the increases the rate of generation of (electron-hole) pairs , And increasing both the Short circuit current (Jsc) and the Open circuit voltages (Voc), thus increases the I-V curve .

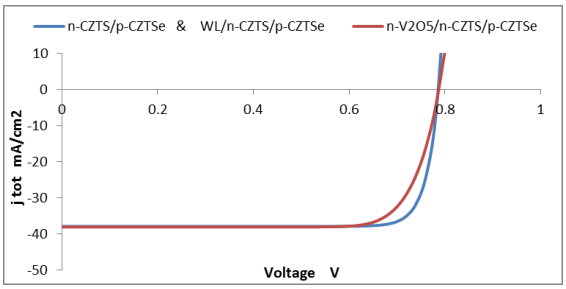

Figure (2) Effect of window layers (WL) on I-V curve

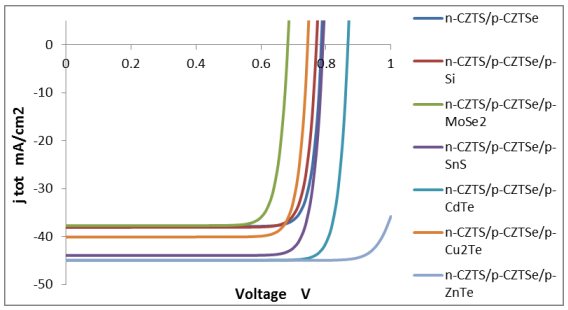

Figure (3) Effect of BSF on I-V curve

Figure (4) shows that the conversion efficiency value (η) is 23.9% at the energy gap (Eg) 2.3 eV for component V_2O_5 , and it increases and constant at approximately 26.5% with the increase in the energy gap (Eg) value for the other window layer (WL) components. As for the Back surface field (BSF), the conversion efficiency value (η) increases from 21.75 to 36% with the increase in the value of the energy gap for it .

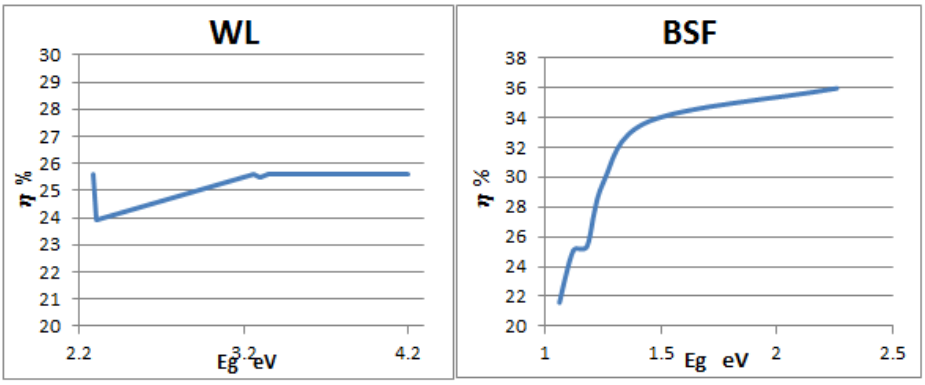

Figure (4) Effect of E_g for WL and BSF layers on η

And for quantum efficiency, Figure (5) affirms that the addition of transition metal oxides (TMO) as a window layer (WL) did not affect the quantum efficiency curve except with V2O5 and the small wavelengths of the rest of the TMO , due to the recombination process when occurring at the front surface of the cell . Figure (6) remarks that the Back surface field (BSF) has an effect on the value of quantum efficiency, where its value decreases when added. It is due to the recombination that occurs at the back surface and the decrease in the absorption level at the long wavelength , And the short length of the spread of the carriers.

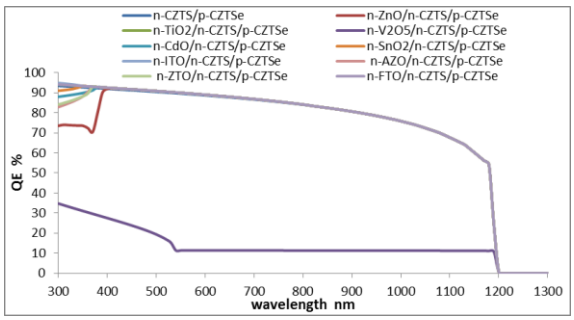

Figure (5) Quantum efficiency (QE) for various window layers (WL)

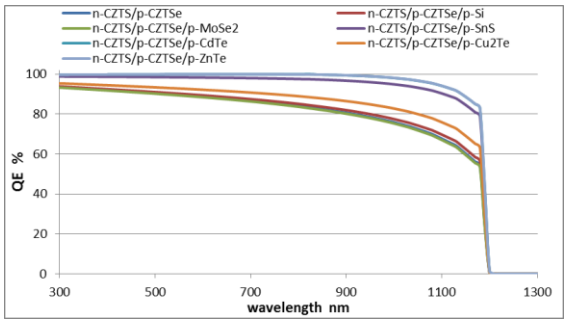

Figure (6) Quantum efficiency (QE) for various BSF

The curve (IV) is one of the most important curves that describes the performance of the solar cell, and Figure (7) points out that the thickness of the absorption layer has a significant effect on the shape of this curve for CdTe, SnS as BSL and TiO_2 , SnO_2 , ITO and FTO as window layers. Increasing the thickness of the absorption layer increases the curve (IV) because the thickness of the absorption layer increasing the absorption coefficient and raise the rate of the generation of pair (electrons - hole), thus increasing the short circuit current Jsc and the voltage of the open circuit Voc, so increasing the curve (IV) in table (3) there is no difference between TMO as

window layer at the same BSF. Therefore, the behavior of I-V curves having same way.

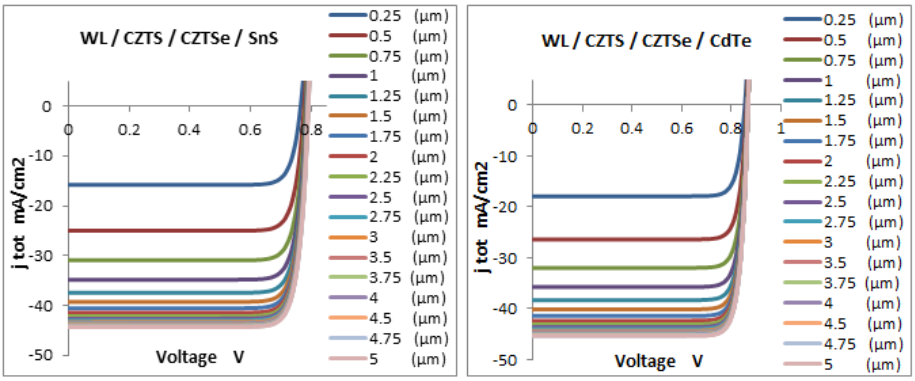

Figure (7) Effect of the thickness of the absorption layer CZTSe on the I-V of the cells

Figure (8) presents Voc values which are increased by rise the thickness of the absorption layer (CZTSe). This rise is due to the increase in the thickness of the absorbent layer and the absorption of more optical photons rise the photo current, which contributes to the generation of pairs (electron - hole) and will rise the value of Voc as equation (1) [19]. This is also the case with Jsc, where the rise is due to the absorption of more photons. However, a linear increase in the Jsc value is observed when the absorption layer thickness is less than 1.5 µm.

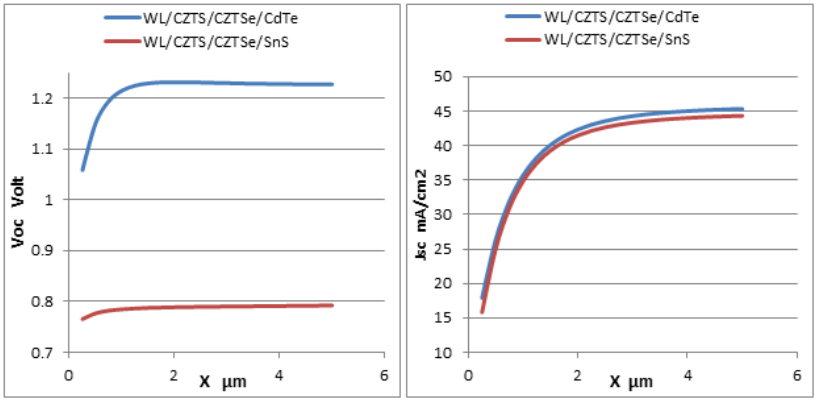

Figure (8) Effect of the thickness of the absorption layer CZTSe on the Open circuit voltage (Voc) and the short circuit current (Jsc) of cells

Figure (9), the value of the FF is reduced by increasing the thickness of the absorption layer. This is due to increase bulk resistance of absorber layer [23]. For conversion efficiency (η), its value is significantly increased when the thickness of the absorption layer is less than 2µm and then begins with a slow increase thereafter. So that the η in CdTe (as BSF) is higher than in SnS and reach 34% at 5 µm thickness of absorption layer which can be explain by absorbed more photons as clear in Fig (10) , Fig (11) .

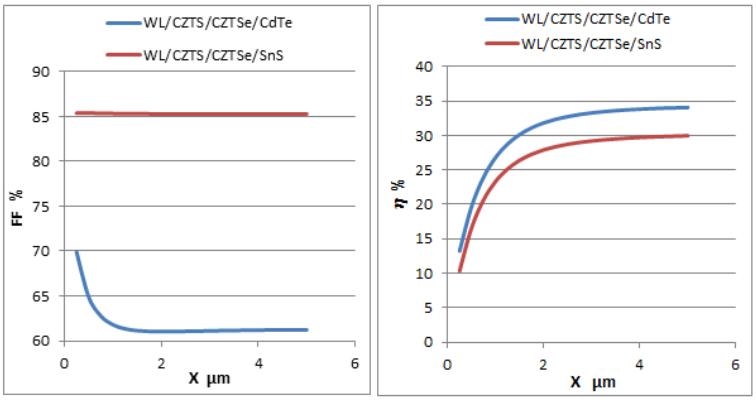

Figure (9) Effect of the thickness of the absorption layer CZTSe on the fill factor (FF) and conversion efficiency (η) of the cells

Quantum efficiency is defined as the percentage between a number of electrons generated to a number of photons absorbed per unit of wavelength falling on the surface of the device and the quantity of the quantum efficiency is one in the case of the ideal binary, ie if a number of electrons generated is equal

to a number of absorbed photons but naturally reflects the light falling at the surface Semiconductor and not all that remains absorbed within the depletion region so the efficiency can be increased by reducing the reflectivity of the surface with an anti-reflective coating such as (SiO2) and the increase in the survival time of the carriers by reducing the structural defects and increase absorption within the depletion area. The main key that plays a significant role in Quantum efficiency is the absorption factor, which It depends on the wavelength [24]. The increase in thickness of the absorption layer affects the value of Quantum efficiency. The higher thickness of the absorbent layer, greater the efficiency value, up to 100%, since the cell is ideal, as in Figs. (10) and (11). In terms of Quantum efficiency it is observed that photons with long wavelengths will absorb deeply into the back absorption layer p-CZTSe, so the Quantum efficiency of the electrons created there is significant and depends on the effect of diffusion .

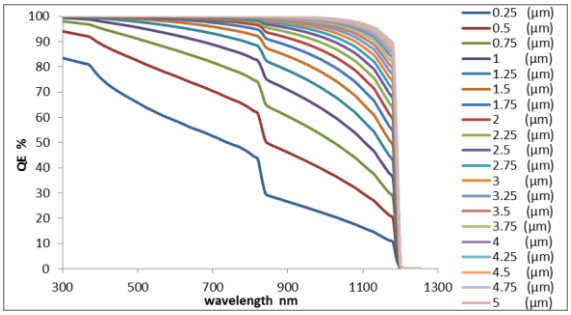

Figure (10) Quantum efficiency curve (QE) for WL/CZTS/CZTSe/CdTe

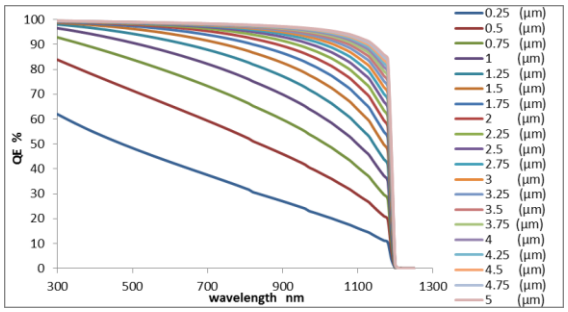

Figure (11) Quantum efficiency curve (QE) for WL/CZTS/CZTSe/SnS

Conclusions

Throughout investigation, the use of software (SCAPS-1D) in the simulation process facilitates the process of manufacturing solar systems and reduce the cost of the study significantly, The transition metal oxides (TiO_2 , SnO_2 , ITO, FTO) showed a slight increase in the efficiency (η) for CZTS / CZTSe from 25. 57% before addition to 25.63% after addition, and the major increase occurred to SnS and CdTe as BSF layer where the efficiency value increased to 29.64%, and 33.75% respectively. Also increase in thickness of the absorption layer CZTSe from the 250 nm to 3µm increasing the efficiency of conversion (η) significantly increased to 30% - 34% (depending on the type of Back surface field) and then start with the approximate stability with the increase in thickness. though increasing the thickness of the absorption layer which is working on a significant can lead to the increase in the quantity of efficiency (QE) and even closer to the value of 100 % .

References

[1] Sze, S.M. (2007). Physics of Semiconductor Devices. 3th edn., library of Congress Cataloging, The United states of America.

[2] Fella, C.M.; Romanyuk, Y. E. and Tiwari, A.N. (2013). Thin-film Photovoltaic Solar Cells. *Solar Energy Materials and Solar Cells*, **119 (1):** 276–277.

[3] Sayed, M. H.; Schoneberg, J.; Parisi, J. and Gutay, L. (2017). Improvement of the structural and electronic properties of CZTSSe solar cells from spray pyrolysis by a CuGe seed layer. *The Royal Society of Chemistry*, **7 (3)** : 20406 – 20411 .

[4] Amu, T.L. and Loreta, T. (2014). Performance optimization of TIN halide perovskite solar cells VIA numerical simulation. 1th edn., African University of Science and Technology: Abuja.

[5] Zhai, H. J. and Wang, L. S. (2002). Electronic structure and chemical bonding of divanadium - oxide clusters (V_2O_X , x =3–7) from anion photoelectron spectroscopy. *The Journal of Chemical Physics journal*, **117 (17)**: 78 - 82 .

[6] Olopade, M. A.; Oyebola, O. O. and Adeleke, B. S. (2012). Investigation of some materials as buffer layer in copper zinc tin sulphide (Cu_2ZnSnS_4) solar cells by SCAPS-1D. *Pelagia Research Library, Advances in Applied Science Research*. **3 (6)**: 3396 - 3400 .

[7] Hossain, M. I.; Alharbi, F.H. and Tabet, N. (2015). Copper oxide as inorganic hole transport material for lead halide perovskite based solar cells. *Solar Energy*, **120 (1)**: 370–380 .

[8] Li, H.; Wang, N. and Liu, X. (2008). Optical and electrical properties of Vanadium doped Indium oxide thin films. *Optics express*, **16 (1)**: 194 – 199 .

[9] Jefferson, P.H. et al. (2008). Band gap and effective mass of epitaxial Cadmium Oxide. *Applied physics letters*, **92 (2)**: 022-101 .

[10] Sivaraman, G. (2003). Characterization Of Cadmium Zinc Telluride Solar Cells. 1st edn., Scholar Commons ,University of South Florida .

[11] Sayed, A. M.; El-Sayed, S.; Morsi, W. M.; Mahrous, S. and Hassen, A. (2014). Synthesis, Characterization, Optical, and Dielectric Properties of Polyvinyl Chloride/Cadmium Oxide Nano composite Films. *Wiley Online Library*, **35 (2)**: 1842-1851 .

[12] Sankrasubramanian, K.; Soundrrajan, P.; Sethuraman, K.; Babu, R.R. and Ramamurthy, K. (2014). Structural optical and electrical properties of transparent conducting hydrophobic cadmium oxide thin films prepared by spray pyrolysis technique. *Super lattices and Microstructures*, **69 (1)** : 29–37.

[13] Anwar, F.; Afrin, S.; Satter, S. S.; Mahbub, R.

and Ulah, S.M. (2017). Simulation and Performance Study of Nanowire CdS/CdTe Solar Cell. *International journal of renewable energy research*, **7(2)**: 885-893.
[14] Mebarkia, C.; Dib, D.; Zerfaoui, H. and Belghit, R. (2016). Energy efficiency of a photovoltaic cell based thin films CZTS by scaps. *Journal of Fundamental and Applied Sciences*, **8(2)**: 363-371.
[15] Zhang, H. et al. (2017). Effect of Zn(O,S) Buffer Layer on Cu_2ZnSnS_4 Solar Cell Performance from Numerical Simulation. *Journal of Applied Science and Engineering*, **20 (1)**: 39 – 46 .
[16] Ngoupo, A. T.; Ouedraogo, S.; Zougmore, F. and Ndjaka, J. M . (2015). New Architecture towards Ultrathin CdTe Solar Cells for High Conversion Efficiency. *International Journal of Photoenergy*, **9 (3)** : 1- 9 .
[17] Chandrasekharan, R. (2012). Numerical modeling of tin-based absorber devices for cost-effective solar photovoltaics. ph.D. thesis, The Pennsylvania State University, Pennsylvania State United States of America .
[18] Altamura, G. (2014). Development of CZTSSe thin films based solar cells. ph.D. thesis. University-Grenoble 1. Grenoble, France .
[19] Lin, p. (2014). Numerical Simulation of Cu_2ZnSnS_4 Based Solar Cells with In_2S_3 Buffer Layers by SCAPS-1D. *Journal of Applied Science and Engineering*, **17 (4)**: 383-390 .
[20] Minbashi, M.; Omrani, M. K.; Memarian, N. and Kim, D. H. (2017). Comparison of theoretical and experimental results for band-gap-graded CZTSSe solar cell. *Current Applied Physics*, **17 (10)**: 1283 - 1243 .
[21] Gunavathy, K. V.; Parthibaraj, V.; Rangasami, C. and Tamilarasan, K . (2016). Prospects of alternate buffer layers for CZTS based thin films solar cells from Numerical Analysis – A Review. *South Asian Journal of Engineering and Technology*, **2 (16)** : 88 – 96 .
[22] Ngoupo, A. T.; Ouedraog, S.; Zougmore, F. and Ndjaka, J. M. (2015). New Architecture towards Ultrathin CdTe Solar Cells for High Conversion Efficiency. *International Journal of Photoenergy*, **9 (8)** : 1-9 .
[23] Nkuissi, J. H. et al. (2015). Optimization of the Output Parameters in Kesterite - based Solar Cells by AMPS-1D. *International Renewable and Sustainable Energy Conference (IRSEC)*, **978 (1)** : 4673-7894 .
[24] Verdeyen, J.T. (1981). Layser Electronics. 4th edn., New York : United States of America.

دراسة تأثير الطبقة النافذة وطبقة BSF على خصائص الخلية الشمسية CZTS / CZTSe باستخدام SCAPS - 1D

علاء حسين نجم ، عايد نجم صالح

قسم الفيزياء , كلية التربية للعلوم الصرفة , جامعة تكريت ، تكريت ، العراق

الملخص

لقد تم دراسة الخلية الشمسية CZTS/CZTSe باستخدام المحاكي الحاسوبي SCAPS-1D, وقد تبين أن زيادة سمك طبقة الإمتصاص p-CZTSe من 250nm إلى 5µm يعمل على زيادة المنحني I-V وبذلك تزداد كل من قيم Voc ، Jsc ، FF ، η حتى تصل إلى 0.79 Volt، 39.35 mA/cm^2 ، 85.92 %، 26.8 % على التوالي، أما الخواص البصرية المتمثلة بالكفاءة الكمية (QE) فتزداد قيمتها من 54% إلى 95%. وبإضافة طبقة أكاسيد العناصر الإنتقالية (TMO) إلى الخلية تبين أنّ الأكاسيد (TiO_2،SnO_2،ITO،FTO) تعطي أعلى كفاءة تحويل بين الأكاسيد الأخرى حيث بلغت 25.63% وتزداد هذه القيمة بزيادة سمك طبقة الإمتصاص حتى تبلغ 29.32%. وبإضافة طبقة الإنعكاس الخلفية (BSF) للخلية وجد أن المركبات p^+-CdTe ، SnS تعطي أعلى كفاءة تحويل حيث بلغت 33.75% ، 29.64% على التوالي ، وزيادة سمك طبقة الإمتصاص يعمل على زيادة قيمة كفاءة التحويل من 13.16% عند السمك 250nm إلى 33.9% عند السمك 5µm للمركب p^+-CdTe ، ومن 10.27% إلى 29.89% للمركب SnS ، بينما تقل قيمة عامل الملئ (FF) من 69.93% عند السمك 250 nm إلى 61.01 % عند السمك 2 µm للمركب p^+-CdTe ، ومن 85.39 % عند السمك 500 nm إلى 85.28 % عند السمك 2.75 µm للمركبSnS . وبجمع هذه المركبات من أكاسيد العناصر الإنتقالية وطبقة الإنعكاس الخلفية مع الخلية CZTS/CZTSe أمكن الحصول على ستة خلايا ذات قيم لكفاءة التحويل تتراوح بين 33.82% و 29.71% وتتغير هذه القيم بتغير سمك طبقة الإمتصاص، وبالنسبة للكفاءة الكمية فتبين أن قيمتها تزداد بزيادة سمك طبقة الإمتصاص حتى تصل إلى 100% عند السمك 5µm وذلك لكون الخلايا مثالية.